Diffusing proteins on a fluctuating membrane: Analytical theory and simulations

Ellen Reister-Gottfried, Stefan M. Leitenberger, and Udo Seifert
II. Institut für Theoretische Physik, Universität Stuttgart, D-70550 Stuttgart, Germany
(Received 26 January 2010; published 4 March 2010)

Using analytical calculations and computer simulations, we consider both the lateral diffusion of a membrane protein and the fluctuation spectrum of the membrane in which the protein is embedded. The membrane protein interacts with the membrane shape through its spontaneous curvature and bending rigidity. The lateral motion of the protein may be viewed as diffusion in an effective potential, hence, the effective mobility is always reduced compared to the case of free diffusion. Using a rigorous path-integral approach, we derive an analytical expression for the effective diffusion coefficient for small ratios of temperature and bending rigidity, which is the biologically relevant limit. Simulations show very good quantitative agreement with our analytical result. The analysis of the correlation functions contributing to the diffusion coefficient shows that the correlations between the stochastic force of the protein and the response in the membrane shape are responsible for the reduction. Our quantitative analysis of the membrane height correlation spectrum shows an influence of the protein-membrane interaction causing a distinctly altered wave-vector dependence compared to a free membrane. Furthermore, the time correlations exhibit the two relevant time scales of the system: that of membrane fluctuations and that of lateral protein diffusion with the latter typically much longer than the former. We argue that the analysis of the long-time decay of membrane height correlations can thus provide a new means to determine the effective diffusion coefficient of proteins in the membrane.

DOI: 10.1103/PhysRevE.81.031903 PACS number(s): 87.16.A−, 87.15.Vv, 87.16.dj

I. INTRODUCTION

Biomembranes are ubiquitous in life, mainly providing spatial compartmentalization. However, a membrane should not be viewed as a mere barrier between different compartments, but serves as a place where a whole variety of functions may take place, such as ion or protein transport, signal transduction, etc. [1]. These functions come about through proteins that move along the membrane. From a physical perspective, the lateral diffusion of the proteins and the shape changes of the membrane caused upon insertion of proteins are among the most interesting issues of these systems.

The recent progress in experimental techniques to measure lateral diffusion coefficients, such as fluorescence correlation spectroscopy [2], single-particle tracking [3], or fluorescence recovery after photobleaching [4], has revealed that many of the functions performed by proteins are crucially influenced by the diffusive behavior of the proteins [5]. Apart from the obvious biological relevance, lateral protein diffusion is also very challenging from a theoretical perspective: compared to diffusion in the bulk, there is a subtlety in the hydrodynamic equations describing the mobility in a two-dimensional fluid since the solution of the two-dimensional Navier-Stokes equation diverges. In order to overcome this so-called Stokes' paradox [6], Saffman and Delbrück [7] considered the mobility of a very thin, rigid object in a narrow almost two-dimensional fluid layer that is surrounded on both sides by a further liquid. This work has received a lot of attention since it is relevant for lateral protein diffusion. While some experiments support their result [8–10], more recent observations for proteins cannot be explained by their theory [11,12].

Another aspect that makes diffusion interesting, particularly in membranes, is that the membrane itself is subject to thermal fluctuations; thus the shape of the membrane is also constantly changing. Methods to analyze shape fluctuations of membranes include off-specular x-ray scattering [13] and video microscopy [14,15]. In the latter method, the contour of a vesicle is detected from optical microscopy records taken at successive time steps. The changes in the contour provide information on the fluctuation spectrum that is used to deduce effective bending rigidities or surface tensions. In a very recent study, Rodríguez-García *et al.* [16] identified the influence of the bilayer nature of a membrane as theoretical calculations [17] have previously predicted. The influence of the density of inclusions embedded in a lipid membrane on the effective bending rigidity was studied by Vitkova *et al.* [18]. In this work, the peptide alamethicin was used as the inclusion. Bassereau and co-workers studied more complicated systems consisting of membranes with inserted proteins and were able to study the altered fluctuation spectrum of a membrane upon activation of the inserted bacteriorhodopsin proteins [19,20].

Theoretically, a bare membrane is well described as a continuous two-dimensional sheet with a bending rigidity and an effective surface tension. This model has been very successful in explaining a whole variety of experimentally observed membrane morphologies [21]. Likewise, membrane shape fluctuations are well captured by this simple model as shown in video microscopy experiments [14,15]. The insertion of additional proteins in a membrane requires an extension of this simple continuous model to include the local interaction of a protein with the membrane. While the influence of thermal membrane fluctuations on the interaction between inclusions has previously been considered in several studies [22,23], the influence on lateral diffusion or the altered membrane height correlations is much less studied. In previous work involving both analytical calculations and simulations, we and others analyzed the geometric effect of measuring the diffusion coefficient from the projected path of the protein [24–26]. While these studies only in-

cluded free diffusion, the lateral diffusion of an inclusion that interacts with the membrane shape is considered in recent studies [24,27–30]. If the membrane shape fluctuations were not influenced by the protein, the effective diffusion coefficient would be *increased* compared to the free diffusion coefficient [24,27,29]. However, this simplifying assumption represents too severe an approximation. By including the backaction of the protein on the membrane fluctuations, Naji *et al.* [30] showed that in equilibrium, the effective lateral diffusion coefficient is *reduced* for which they were able to give an approximate expression. Parts of the current work are complementary to their study.

On a more collective level, the interaction between membrane and embedded proteins can cause morphological changes. Leibler [31] studied a model with a protein density field that induces a spontaneous curvature capable of causing an instability of the membrane. He finds two characteristic time scales for membrane fluctuations, with one of them potentially unstable in a certain wave-vector range. Related work by Bivas and Méléard [32] on bending elasticity and fluctuations of spherical bilayer vesicles with additives reveals an additional characteristic time scales. In their work, the bilayer membrane comprises two individual sheets such that the third time scale results from the friction between the two layers.

Divet *et al.* [33] studied an extension of Leibler's work that allows an exchange of proteins between the membrane and the surrounding fluid. Depending on the considered length scale, they find several relevant time scales for membrane height and density fluctuations. Surprisingly, this relevance of different time scales in membrane height correlations has, to the best of our knowledge, not been previously observed in experiments.

In the present work, we study the two interrelated effects following from a protein-membrane interaction: the reduction of the lateral diffusion coefficient of the protein and the modifications of the static and time-dependent height correlation functions of the membrane. In our study, the additional energy caused by the insertion of the protein arises from an effective bending rigidity and spontaneous curvature of the protein. The dynamics of our system is dominated by two processes: the shape fluctuations of the membrane and the lateral diffusion of the protein. Taking into account the hydrodynamic interaction of a membrane with the surrounding fluid, we are able to derive a Langevin equation for the dynamics of the membrane shape, which becomes a function of the protein's position. Lateral diffusion of the protein is captured by another Langevin equation that takes into account the shape of and the interaction with the membrane. These two coupled equations of motions are the starting point for our analytical calculations and their numerical integration make out our simulation scheme.

Using a systematic approach, we present two main results for lateral diffusion: we argue that in equilibrium, the effective lateral diffusion coefficient of a protein that interacts with the membrane shape is universally decreased compared to the free diffusion coefficient applicable if no interactions were present. Beyond this general argument we, furthermore, derive an explicit expression for the effective diffusion coefficient of a protein with spontaneous curvature and bending rigidity by applying a path-integral approach. To lowest order, our expression agrees with that recently derived by Naji *et al.* [30] through an estimate of the power loss of the diffusing protein in the limit that the membrane shape minimizing the system's energy instantaneously tracks the protein's position. Our approach reveals that their expression resulting from a phenomenological approximation formally corresponds to the lowest order of an expansion in $(\beta\kappa)^{-1}$ using $\beta \equiv (k_B T)^{-1}$, with temperature T, Boltzmann's constant k_B, and bending rigidity κ of the membrane.

We compare results of our simulation scheme to this lowest-order expression and find good quantitative agreement. Several correlation functions contribute to the effective diffusion coefficient. The quantitative analysis of these contributions from our simulation results shows that the correlations between the response of the membrane and the preceding stochastic force acting on the protein effectively reduce the diffusion coefficient, while all other contributions would cause an increase.

Concerning the altered membrane spectrum, we analytically develop an approximate expression for the height correlation function applicable for equal bending rigidity of protein and membrane. In the limit of slow protein diffusion compared to membrane fluctuations, we find two time regimes for the decay of height correlations: at small times, the decay is dominated by membrane dynamics, while the diffusive time scale of the protein becomes the only relevant time scale at later times. Since we find this feature in the simulations not only for equal bending rigidities of membrane and protein, we suggest that the experimental analysis of the late decay of dynamical membrane height correlations can provide a means to determine the effective diffusion coefficient of proteins in the membrane. To corroborate this argument, we use our model to give a rough estimate suggesting that the effect should be visible in realistic systems.

The paper is organized as follows. In the next section, we present the model of the system and develop the equations of motion both for the protein and the membrane. In the limit of small ratios of temperature and bending rigidity, these are then used in Secs. III A and III B to develop an exact analytical expression for the effective lateral diffusion coefficient and for the dynamical membrane height correlations, respectively. In Sec. IV A, we briefly explain our simulation scheme and motivate the parameters used in the simulations. In Sec. IV B, we show that the derived analytical expression for the effective diffusion coefficient shows good agreement with simulations using parameters of typical experiments. We, furthermore, quantitatively analyze the correlation functions that contribute to the diffusion coefficient. The membrane height correlations are compared to our analytical expressions in Sec. IV C. In Sec. V, we show the determination of the effective diffusion coefficient from the late time decay of height correlations and discuss that this procedure should be experimentally feasible in realistic system. We finally close with some conclusions.

II. MODEL

In our model, we consider a single diffusing inclusion in a membrane with bending rigidity κ that we describe in the

Monge gauge. The small inclusion with radius a_p has a spontaneous curvature C_p and its stiffness may differ from that of the membrane by a factor of γ. The energy of the system of size L^2 may be expressed by

$$\mathcal{H}[h,\mathbf{R}] = \frac{\kappa}{2}\int_{L^2} d^2r\{(\nabla_{\mathbf{r}}^2 h)^2 + \pi a_p^2 G(\mathbf{r}-\mathbf{R}) \times[\gamma(\nabla_{\mathbf{r}}^2 h - C_p)^2 - (\nabla_{\mathbf{r}}^2 h)^2]\}, \quad (1)$$

with the height function $h(\mathbf{r})$ that quantifies the distance between the membrane and the position $\mathbf{r}$ on a flat reference plane. The particle position projected onto this plane is given by $\mathbf{R}$. The function $G(\mathbf{r}-\mathbf{R})$ defines a weighting function of the particle that must fulfill the normalization $\int_{L^2} d^2r G(\mathbf{r})=1$. In our simulations, we set the weighting function to a Gaussian $G(r)=(\pi a_p^2)^{-1}\exp[-r^2/a_p^2]$ such that the transition from membrane to particle is smooth. If we use the Fourier expansions $h(\mathbf{r})=\frac{1}{L^2}\Sigma_{\mathbf{k}} h(\mathbf{k})\exp(i\mathbf{k}\cdot\mathbf{r})$ and $h(\mathbf{k}) = \int_{L^2} d^2r h(\mathbf{r})\exp(-i\mathbf{k}\cdot\mathbf{r})$, the Hamiltonian becomes

$$\mathcal{H}[h(\mathbf{k}),\mathbf{R}] = \frac{\kappa}{2}\left\{\frac{1}{L^2}\sum_{\mathbf{k}} k^4 h(\mathbf{k})h(-\mathbf{k}) + (\gamma-1)\frac{\pi a_p^2}{L^4}\sum_{\mathbf{k},\mathbf{k}'} k^2 k'^2 G(-\mathbf{k}-\mathbf{k}')e^{i(\mathbf{k}+\mathbf{k}')\cdot\mathbf{R}}h(\mathbf{k})h(\mathbf{k}') + 2\gamma C_p\frac{\pi a_p^2}{L^2}\sum_{\mathbf{k}} k^2 G(-\mathbf{k})e^{i\mathbf{k}\cdot\mathbf{R}}h(\mathbf{k})\right\} + \gamma\pi a_p^2 C_p^2. \quad (2)$$

From this Hamiltonian, it is in principle possible to numerically calculate the equilibrium height correlations $\langle h(\mathbf{k})h(\mathbf{k}')\rangle$ applying methods used in [34]. While these methods are restricted to time-independent equilibrium quantities, our simulation scheme, described later in the paper, allows us to not only obtain these quantities but also time-dependent information. For the special case that both the protein and the membrane have the same bending rigidity, i.e., $\gamma=1$, the height correlations are given by

$$\langle h(\mathbf{k})h(-\mathbf{k})\rangle = \frac{L^2}{k^4}\left[\frac{1}{\beta\kappa} + \rho\pi a_p^2 C_p^2 G(\mathbf{k})G(-\mathbf{k})\right], \quad (3)$$

with the ratio of protein area to system size

$$\rho \equiv \pi a_p^2/L^2. \quad (4)$$

While Eq. (3) is derived for a single protein on the membrane, the extension to several noninteracting proteins would lead to the same result with ρ resembling the overall area density of the proteins. Compared to the free membrane without protein, whose height correlations are given by the first term, the protein gives rise to an *additive* term that depends on the various parameters characterizing the particle. Following previous studies [31–33], it is possible to define a k-dependent effective bending rigidity $\kappa_{\text{eff}}(k)$ such that the spectrum of the membrane has the form of a protein-free membrane $\langle h(\mathbf{k})h(-\mathbf{k})\rangle_{\text{free}}=L^2/[\beta\kappa_{\text{eff}}(k)k^4]$. This leads to

$$\frac{\kappa_{\text{eff}}(k)}{\kappa} = [1+\beta\kappa\rho\pi a_p^2 C_p^2 G(\mathbf{k})G(-\mathbf{k})]^{-1}. \quad (5)$$

Note that the addition of the protein in the membrane always leads to a reduction of the effective bending rigidity of the system as has been pointed out previously when inclusions are inserted into a membrane [31]. However, the effective bending rigidity cannot become negative, hence the membrane not unstable.

Neglecting any geometric effects caused by the projection of the protein path, which we have previously determined to be rather small for realistic membranes [24], the diffusive motion of the protein and the thermal fluctuations of the membrane, i.e., the dynamics of the height modes $h(\mathbf{k},t)$, are appropriately described by the following coupled Langevin equations:

$$\dot{\mathbf{R}}(t) = -\mu_p\nabla_{\mathbf{R}}\mathcal{H} + \boldsymbol{\zeta}(t), \quad (6)$$

$$\dot{h}(\mathbf{k},t) = -\Lambda(k)\frac{\delta\mathcal{H}}{\delta h(\mathbf{k},t)} + \xi(\mathbf{k},t), \quad (7)$$

with the stochastic forces $\boldsymbol{\zeta}(t)$ and $\xi(\mathbf{k},t)$ that are related to the mobilities $\mu_p \equiv D_p/k_BT$ of the protein [35] and $\Lambda(k)$ of the membrane, respectively, via the fluctuation-dissipation theorems

$$\langle\zeta_l(t)\rangle = 0,$$

$$\langle\zeta_l(t)\zeta_m(t')\rangle = 2D_p\delta_{l,m}\delta(t-t') \quad (8)$$

and

$$\langle\xi(\mathbf{k},t)\rangle = 0,$$

$$\langle\xi(\mathbf{k},t)\xi(\mathbf{k}',t')\rangle = 2k_BT\Lambda(k)L^2\delta_{\mathbf{k}',-\mathbf{k}}\delta(t-t'). \quad (9)$$

The mobility of the membrane takes into account the dynamics of the membrane caused by the surrounding fluid. A hydrodynamical derivation involving the Oseen tensor leads to a mobility of $\Lambda(k)=(4\eta k)^{-1}$ for the undulations $k\neq 0$, with the viscosity η of the surrounding fluid [21]. For $k=0$, i.e., the center of mass movement of the membrane, we set $\Lambda(k=0)=0$ since it does not influence the properties of interest in our study.

III. ANALYTICAL APPROACH

A. Diffusion coefficient D_{eff}

We derive an analytical expression for the effective diffusion coefficient D_{eff} by exploiting that for biomembranes typically $(\beta\kappa)^{-1} \ll 1$. We first determine the minimum of the energy (2). The condition $\frac{\partial \mathcal{H}}{\partial h(\mathbf{k})}\big|_{\hat{h}_{\mathbf{k}}}=0$ leads to the equation

$$0 = k^2 \hat{h}_{-\mathbf{k}} + (\gamma - 1)\rho \sum_{\mathbf{k}'} k'^2 G(\mathbf{k}+\mathbf{k}') \exp[i(\mathbf{k}+\mathbf{k}')\cdot \mathbf{R}] \hat{h}_{\mathbf{k}'} + \gamma C_p \pi a_p^2 G(\mathbf{k}) \exp(i\mathbf{k}\cdot\mathbf{R}) \tag{10}$$

for the height modes $\hat{h}_{\mathbf{k}}$ that minimize the energy. Using the ansatz $\hat{h}_{\mathbf{k}} = \frac{B_{\mathbf{k}}}{k^2} \exp(-i\mathbf{k}\cdot\mathbf{R})$, the energy is minimal for

$$B_{\mathbf{k}} = -\gamma C_p \pi a_p^2 \sum_{\mathbf{q}} M^{-1}_{\mathbf{k},\mathbf{q}} G(\mathbf{q}), \tag{11}$$

with the matrix

$$M_{\mathbf{k},\mathbf{q}} \equiv \delta_{\mathbf{k},\mathbf{q}} + (\gamma - 1)\rho G(\mathbf{q}+\mathbf{k}). \tag{12}$$

Inserting this result into the Hamiltonian shows that the energy minimum does not depend on the particle position as expected from the isotropy of the particle position.

The first question we will address is whether the effective diffusion constant is larger or smaller than the free diffusion coefficient D_p applicable without coupling, i.e., $\gamma=0$. The degrees of freedom in the Hamiltonian (2) are given by the membrane modes $h(\mathbf{k})$ and the position $\mathbf{R}$ of the protein. Due to the appearance of the membrane modes up to quadratic order in the Hamiltonian, the thermal averages $\langle |h(\mathbf{k})|^2 \rangle$ remain bounded. The position of the protein, however, is not bounded, such that diffusive motion is possible. Effectively, the protein moves in a time-dependent periodic potential given by the height modes $h(\mathbf{k},t)$. Diffusion in periodic potentials has been previously considered in a large number of studies. If the particle is only subject to the potential and no other external force, it is easily shown that the effective diffusion coefficient of the particle is always smaller than or equal to the free diffusion coefficient [36,37]. Thus we conclude that the effective diffusion coefficient D_{eff} of a protein whose interaction with the membrane depends on the shape obeys

$$D_{\mathrm{eff}} \leq D_p \tag{13}$$

in all situations without external driving forces.

While we know that the diffusion coefficient is in general reduced due to the membrane, we will derive an explicit analytical expression to quantify the effect for our model, the validity of which we will discuss and analyze through simulations. A quick glance at the Langevin equations (6) and (7) shows that they are highly nonlinear such that the exact solution is not straightforward. In order to develop an expression for D_{eff}, we must, therefore, apply certain approximations.

In a path-integral description [38], the probability distribution $\mathcal{P}$ of the paths $\mathbf{R}(t)$ of the diffusing protein and of the height modes $h(\mathbf{k},t)$ follows from the weight of noise fluctuations and is given by the functional

$$\mathcal{P}[\mathbf{R}(t), h(\mathbf{k},t)] \sim \exp\left\{ -\frac{1}{2k_B T} \int_0^t d\tau L[\mathbf{R}(\tau), h(\mathbf{k},\tau)] \right\}, \tag{14}$$

with the function

$$L(\mathbf{R}, h(\mathbf{k})) = \frac{1}{2\mu_0} (\dot{\mathbf{R}} + \mu_0 \nabla_{\mathbf{R}} \mathcal{H})^2 + \sum_{\mathbf{k}} \frac{1}{2\Lambda(k)} \left| \dot{h}(\mathbf{k}) + \Lambda(k) \frac{\partial \mathcal{H}}{\partial h(\mathbf{k})} \right|^2. \tag{15}$$

If we introduce the deviation

$$y_{\mathbf{k}} \equiv h(\mathbf{k}) - \hat{h}_{\mathbf{k}}[\mathbf{R}(t)] \tag{16}$$

of the membrane shape from the instantaneous membrane shape that minimizes the energy of the system the Hamiltonian may approximately be written in the form

$$\mathcal{H} = \mathcal{H}_0 + \frac{1}{2} \sum_{\mathbf{k},\mathbf{k}'} y_{\mathbf{k}} \left. \frac{\delta^2 \mathcal{H}}{\delta h(\mathbf{k}) \delta h(\mathbf{k}')} \right|_{\hat{h}_{\mathbf{k}}(\mathbf{R})} y_{\mathbf{k}'}, \tag{17}$$

where $\mathcal{H}_0 \equiv \mathcal{H}[\hat{h}(t)]$ is the energy minimum. Since the second functional derivative of the energy with respect to the height is proportional to the bending rigidity κ, it is convenient to define

$$\beta\kappa V_{\mathbf{k},\mathbf{k}'}(\mathbf{R}) \equiv \left. \frac{\delta^2 \mathcal{H}}{\delta h(\mathbf{k}) \delta h(\mathbf{k}')} \right|_{\hat{h}_{\mathbf{k}}(\mathbf{R})}. \tag{18}$$

Up to total derivatives leading only to boundary terms, we can then rewrite the function L as a function of $\mathbf{R}$ and $y_{\mathbf{k}}$,

$$\begin{aligned} L[\mathbf{R}, y(\mathbf{k})] = {} & \frac{1}{2\mu_0} \dot{\mathbf{R}}^2 + \sum_{\mathbf{k}} \frac{1}{2\Lambda(k)} [|(\dot{\mathbf{R}}\cdot\nabla_{\mathbf{R}})\hat{h}_{\mathbf{k}}|^2 \\ & + 2\dot{y}^*_{\mathbf{k}} (\dot{\mathbf{R}}\cdot\nabla_{\mathbf{R}})\hat{h}_{\mathbf{k}} + |\dot{y}_{\mathbf{k}}|^2] \\ & + \frac{1}{2} \Bigg\{ \mu_0 (\beta\kappa)^2 \Bigg[\sum_{\mathbf{k},\mathbf{k}'} (y_{\mathbf{k}} \nabla_{\mathbf{R}} V_{\mathbf{k},\mathbf{k}'} y_{\mathbf{k}'} \\ & - y_{\mathbf{k}} V_{\mathbf{k},\mathbf{k}'} \nabla_{\mathbf{R}} \hat{h}_{\mathbf{k}'}) \Bigg]^2 + \frac{1}{2} (\beta\kappa)^2 \sum_{\mathbf{k}} \Lambda(\mathbf{k}) \\ & \times \left(\sum_{\mathbf{k}'} V_{\mathbf{k},\mathbf{k}'} y_{\mathbf{k}'} \right)^2 \Bigg\}. \end{aligned} \tag{19}$$

To determine the effective mobility of the particle, it would be necessary to integrate out the deviation y in the probability distribution $\mathcal{P}$. Since this cannot be done explicitly, we employ a saddle-point approximation, i.e., we replace all the possible paths $y_{\mathbf{k}}(t)$ with the path $\tilde{y}_{\mathbf{k}}(t)$ that minimizes the function L and hence contributes to the probability distribution (14) the most. The path $\tilde{y}_{\mathbf{k}}(t)$ follows from the Euler-Lagrange equations

$$\frac{d}{dt}\frac{\partial L}{\partial \dot{\tilde{y}}_{\mathbf{k}}} - \frac{\partial L}{\partial \tilde{y}_{\mathbf{k}}} = 0. \tag{20}$$

As before, we assume that only small variations $\tilde{y}_{\mathbf{k}}$ in the height are relevant allowing us to linearize the resulting differential equations

$$\frac{1}{\Lambda(\mathbf{k})}\ddot{\tilde{y}}_{\mathbf{k}}(t) - (\beta\kappa)^2 \sum_{\mathbf{k}''} \Lambda(\mathbf{k}'')\left(\sum_{\mathbf{k}'} V_{\mathbf{k}'',\mathbf{k}'}\tilde{y}_{\mathbf{k}'}\right)V_{\mathbf{k}'',\mathbf{k}} - \mu_0(\beta\kappa)^2\left(\sum_{\mathbf{k}'',\mathbf{k}'} \nabla_{\mathbf{R}}\hat{h}_{\mathbf{k}'}V_{\mathbf{k}'',\mathbf{k}'}\tilde{y}_{\mathbf{k}''}\right)\sum_{\mathbf{k}'} V_{\mathbf{k},\mathbf{k}'}\nabla_{\mathbf{R}}\hat{h}_{\mathbf{k}'} = -\frac{1}{\Lambda(\mathbf{k})}\frac{d^2\hat{h}_{\mathbf{k}}[\mathbf{R}(t)]}{dt^2} \tag{21}$$

or, in a simplified notation,

$$\ddot{\tilde{y}}_{\mathbf{k}}(t) - (\beta\kappa)^2 \sum_{\mathbf{k},\mathbf{k}'} A_{\mathbf{k},\mathbf{k}'}\tilde{y}_{\mathbf{k}'} = -\frac{d^2\hat{h}_{\mathbf{k}}[\mathbf{R}(t)]}{dt^2}, \tag{22}$$

using the positive-definite matrix $A_{\mathbf{k},\mathbf{k}'}$. The homogeneous solution of this equation is a simple relaxation on time scales proportional to $(\beta\kappa)^{-1}$ and plays, therefore, a minor role for large values of $\beta\kappa$. We are now interested in the significance of the bending rigidity κ on the inhomogeneous solution. To this end, we drop all dependencies of $\mathbf{k}$ in Eq. (22) as though the system only had a single wave mode without altering the order of $\beta\kappa$. The inhomogeneous solution is then given by

$$\tilde{y}_{\mathrm{inh}}(t) = \frac{1}{2\beta\kappa\sqrt{A}}\int_0^t d\tau\left(e^{\beta\kappa\sqrt{A}(t-\tau)} - e^{\beta\kappa\sqrt{A}(\tau-t)}\right)\frac{d^2\hat{h}}{d\tau^2}. \tag{23}$$

For large $\beta\kappa$ and slow protein diffusion, the membrane shape minimizing the energy $\hat{h}[\mathbf{R}(t)]$ only weakly changes on the relaxation-time scale. Hence, membrane shape deviations $\tilde{y}_{\mathbf{k}}$ are of the order $\mathcal{O}[(\beta\kappa)^{-2}]$. Inserting this result into Eq. (19) and keeping only leading orders of $(\beta\kappa)^{-1}$, we arrive at

$$L[\mathbf{R},\tilde{y}(\mathbf{k})] = \frac{1}{2\mu_0}\dot{\mathbf{R}}^2 + \sum_{\mathbf{k}}\frac{1}{2\Lambda(k)}|(\dot{\mathbf{R}}\cdot\nabla_{\mathbf{R}})\hat{h}_{\mathbf{k}}|^2 + \mathcal{O}[(\beta\kappa)^{-2}]. \tag{24}$$

It is now possible to identify an effective diffusion coefficient D_{eff} for the diffusing protein from the prefactor of the $\dot{\mathbf{R}}^2$ term

$$\frac{D_0}{D_{\mathrm{eff}}} = 1 + \sum_{\mathbf{k}}\frac{\mu_0}{\Lambda(k)}|\nabla_{\mathbf{R}}\hat{h}_{\mathbf{k}}|^2 = 1 + \sum_{\mathbf{k}}\frac{\mu_0}{\Lambda(k)}\frac{B_{\mathbf{k}}B_{-\mathbf{k}}}{k^2}, \tag{25}$$

with $B_{\mathbf{k}}$ from Eq. (11) and using isotropy in the x and y directions of the system. This systematic derivation of an analytical expression for the diffusion of a protein that interacts with the membrane shape constitutes our first main result. The analysis of experiments with both model and biological membranes shows that $(\beta\kappa)^{-2}$ is typically smaller than 0.01, hence, sufficiently small to expect a wide applicability of this expression. The first line of this expression agrees with the result of Naji *et al.* [30]. In their derivation, they apply an adiabatic approximation assuming the membrane shape to instantaneously follow the path of the protein. The effective diffusion coefficient is then derived from an estimation of the power loss of the diffusing particle. Our derivation identifies their approximate result as the lowest order of an expansion in $(\beta\kappa)^{-1}$.

After the general solution for the effective diffusion coefficient, we will now turn to the special case of a protein with a weighting function expressed through Dirac's delta function $G(\mathbf{R}-\mathbf{r})=\delta(\mathbf{R}-\mathbf{r})$. In this case, the Fourier transform of G is independent of the wave vector $\mathbf{k}$, such that $G(\mathbf{k})=1$. This leads to the height mode

$$\hat{h}_{\mathbf{k}}(\mathbf{R}) = -\frac{1}{k^2}\frac{\gamma C_p\pi a_p^2}{1+(\gamma-1)\rho\sum_{\mathbf{k}'}1}\exp(-i\mathbf{k}\cdot\mathbf{R}), \tag{26}$$

minimizing the free energy $\mathcal{H}$. The resulting energy minimum is

$$\mathcal{H}[\hat{h}] = \frac{\kappa}{2}\gamma\pi a_p^2 C_p^2\frac{1}{1+\gamma\rho\left(\sum_{\mathbf{k}}1\right)/\left(1-\rho\sum_{\mathbf{k}}1\right)}. \tag{27}$$

Following the above procedure but now inserting the special choice for the weighting function leads to the effective diffusion coefficient

$$\frac{D_0}{D_{\mathrm{eff}}} = 1 + \sum_{\mathbf{k}}\frac{\mu_0}{\Lambda(k)}\frac{1}{k^2}\frac{\gamma^2 C_p^2\pi^2 a_p^4}{\left(1+(\gamma-1)\rho\left(\sum_{\mathbf{k}'}1\right)\right)^2}. \tag{28}$$

In the next step, we will evaluate the sums over all possible wave vectors $\mathbf{k}$. On one hand, the smallest value of the x or y component is defined by the system size, $k_{x,\min}=2\pi/L$, and is thus approximately zero for large systems. On the other hand, the largest value $k_{x,\max}=2\pi/a_c$ is limited by a microscopic cutoff length a_c that corresponds to the size of the lipids. Thus the expression $\rho\Sigma_{\mathbf{k}}1$ in the denominator of Eq. (28) leads to $\pi a_p^2/a_c^2$ using the definition of ρ given in Eq. (4). The evaluation of the other sum over $\mathbf{k}$ depends on the specific form of the membrane mobility. Using $\Lambda(k)=(4\eta k)^{-1}$ makes the evaluation of $\Sigma_{\mathbf{k}}k^{-1}$ necessary, such that the expression for the ratio of the diffusion coefficients becomes

$$\frac{D_0}{D_{\mathrm{eff}}} = 1 + \frac{\mu_0 4\eta\gamma^2 C_p^2\pi a_p^4}{\left[1+(\gamma-1)\frac{a_p^2}{a_c^2}\right]^2}\ln\left(\frac{\sqrt{2}+1}{\sqrt{2}-1}\right)\frac{L^2}{a_c}. \tag{29}$$

Typically, the stiffness of a diffusing protein will be significantly larger than that of the membrane. In the limit $\gamma\gg 1$, the resulting effective diffusion coefficient is given by the relation

$$\frac{D_0}{D_{\mathrm{eff}}} = 1 + \mu_0 4\eta C_p^2\pi\ln\left(\frac{\sqrt{2}+1}{\sqrt{2}-1}\right)L^2 a_c^3. \tag{30}$$

Equation (28) shows that a nonzero spontaneous curvature C_p is crucial in order to have an influence on the diffusion coefficient of the protein. Within our model, a mere differ-

ence in the bending rigidity of the membrane and the protein, i.e., $\gamma \neq 1$, does not lead to an altered diffusion coefficient.

Before testing our expression by comparing it to simulations, we will discuss two limiting cases for Eq. (28). Without altering the general conclusions, we will give this discussion only for a single k mode. As was expected, our expression reveals an effective diffusion coefficient that always has an upper bound of D_0. For very small ratios μ_0/Λ [$\Lambda \equiv \Lambda(k)$], i.e., if the membrane is much more mobile than the protein, the reduction of the effective diffusion coefficient is linear in this ratio $D_{\mathrm{eff}}/D_0 \approx 1-|B_{\mathbf{k}}|^2\mu_0/\Lambda$. The free mobility of the protein dominates its effective movement. The influence of the membrane is weak since it can adjust quickly to the position of the protein. In this situation, our approximation that the system's energy is always close the minimum is fulfilled and our expression will serve as a very good estimate. For the limit in which the membrane moves much slower than the particle, which corresponds to the scenario of diffusion in an (almost) fixed periodic potential, our expression predicts the asymptotic behavior $D_{\mathrm{eff}}/D_0 \approx |B_{\mathbf{k}}|^{-2}\Lambda/\mu_0$. Thus the movement of the protein is mainly dominated by the membrane mobility such that it is strongly slowed down. However, if the diffusing particle effectively sees a fixed energy landscape, the stochastic motion enables the protein to hop from one energy minimum to another, such that our previous approximation that the protein always stays very close to the position of the instantaneous energy minimum may no longer be valid.

B. Temporal decay of membrane height correlations

Using the equations of motion (6) and (7), a calculation of the full height correlation function $\langle h(\mathbf{k},t)h(\mathbf{k}',t')\rangle$ is not feasible analytically. We rather determine this quantity from our simulation scheme. Nevertheless, in order to gain an understanding of the possible contributions to the correlation function, it is instructive to consider the special case of equal bending rigidities of the particle and the membrane, $\gamma=1$. The general solution of the Langevin Eq. (7) is then given by

$$h(\mathbf{k},t) = h(\mathbf{k},0)e^{-t/\tau_M(k)} + e^{-t/\tau_M(k)}\int_0^t dt' e^{t'/\tau_M(k)}\left[\xi(\mathbf{k},t') - \frac{C_p \pi a_p^2 G(\mathbf{k})}{k^2 \tau_M(k)} e^{-i\mathbf{k}\cdot\mathbf{R}(t')}\right], \tag{31}$$

with the k-dependent membrane time scale

$$\tau_M(k) \equiv 4\eta/(\kappa k^3). \tag{32}$$

Using the fluctuation-dissipation theorem (9) and assuming that the particle diffuses on time scales much larger than $\tau_M(k)$, the height correlation function is given by

$$\langle h(\mathbf{k},t)h(-\mathbf{k},t')\rangle = \frac{L^2}{\beta\kappa k^4}\left[e^{-|t-t'|/\tau_M(k)} + \beta\kappa\rho\pi a_p^2 C_p^2 G(\mathbf{k})G(-\mathbf{k})e^{-|t-t'|/\tau_D(k)}\right], \tag{33}$$

with the diffusive time scale

$$\tau_D(k) \equiv (D_{\mathrm{eff}}k^2)^{-1}. \tag{34}$$

In order to arrive at Eq. (33), we use $\langle \exp\{-i\mathbf{k}\cdot[\mathbf{R}(t)-\mathbf{R}(t')]\}\rangle = e^{-|t-t'|/\tau_D(k)}$ which follows for diffusive motion of the protein with an effective diffusion coefficient D_{eff}.

Equation (33) shows that the dynamics of the height correlation function of the membrane is determined by the two time scales present in the system: the membrane time scale $\tau_M(k)$ and the diffusive time scale $\tau_D(k)$. Our calculations assumed $\tau_M(k) < \tau_D(k)$, thus, the decay of height correlations for small times $t-t'$ will be dominated by the membrane dynamics while for large times, the diffusion of the particle takes over. While our calculation is strictly valid only in the case of $\gamma=1$, the qualitative behavior persists also for the case $\gamma \neq 1$ as will be shown when we present simulation results. Note that the naive usage of an effective binding rigidity $\kappa_{\mathrm{eff}}(k)$ would lead to a single time scale for each mode k. Since the properties of the system are clearly dominated by two time scales, the concept of $\kappa_{\mathrm{eff}}(k)$ is only applicable for properties that are not time dependent.

IV. SIMULATIONS

A. Scheme

Our simulation scheme comprises the numerical integration of the two coupled Langevin equations (6) and (7). However, the equation of motion given for the protein in Eq. (6) neglects that the particle actually diffuses along the membrane, in other words a curved surface. The shape of the membrane influences the Langevin equation, the exact form of which is given in Refs [25,27], and used in our simulations. Thus the free diffusion coefficient D_0 used in the simulations is slightly larger than the value of D_p in Eq. (6) [35].

The membrane is mapped on a square $N \times N$ lattice such that the length of the system is $L=N\ell$ with the lattice spacing ℓ. The membrane shape is evolved in time by a time discrete version of Eq. (7) in Fourier space. This part of the scheme is an extension of the Fourier space Brownian dynamics simulation method introduced by Lin and Brown [39–41].

After every update of the membrane shape, the position of the particle is altered by using a discrete version of Eq. (6). However, the particle's position is not evolved on the lattice. The membrane height at the particle position that enters in the equation of motion is determined through linear extrapolation from the height at the four nearest-neighbor lattice sites. The shape of the membrane in real space $h(\mathbf{r},t)$ is determined by use of fast Fourier transforms implementing the FFTW library [42]. For a more detailed account of the simulation scheme we refer the reader to refs [25,27].

All simulation results presented in this paper were performed on a 64×64 lattice with a lattice spacing of $\ell = 10$ nm. The radius of the protein is set to $a_p = 2\ell$. The fluid surrounding the membrane is water with a viscosity of $\eta = 10^{-3}$ kg/(ms) or $\eta = 2.47 \times 10^{-7}$ s/$(\beta\ell^2)$ in the units of our model at $T=300$ K. The discrete integrations of both membrane shape and particle position are performed with a time step of $\Delta t = 10^{-9}$ s that is significantly smaller than the smallest time scale $\tau_{M,\mathrm{min}}$ in the system. If not stated otherwise, the diffusion coefficient of the protein is set to $D_0 = 5$

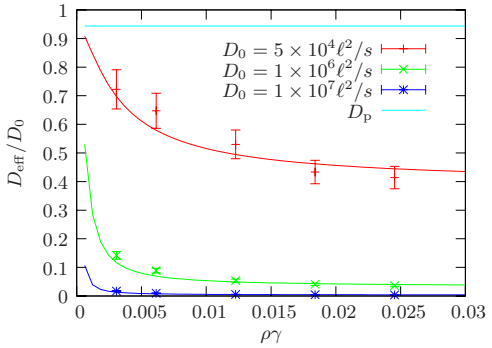

FIG. 1. (Color online) Ratio $D_{\rm eff}/D_0$ as a function of the coupling coefficient $\rho\gamma$ for the given free diffusion coefficients D_0 in units of ℓ^2/s. The bending rigidity of the membrane is $\beta\kappa=5$ and the spontaneous curvature of the protein $C_p\ell=1$.

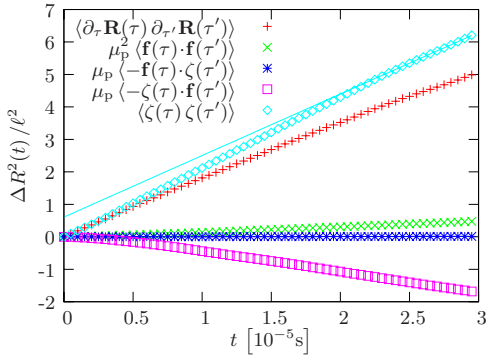

FIG. 2. (Color online) Force correlations integrated twice in time to show the respective contribution to the mean squared displacement of the protein for $\gamma=1$ and $C_p\ell=1$. The results apply for $\tau\leq\tau'$.

$\times 10^{-8}\ \mathrm{cm}^{-2}/\mathrm{s}=5\times10^4\ell^2/\mathrm{s}$. This ensures that the membrane time scale is always smaller than the diffusive time scale $\tau_M(k)<\tau_D(k)$ as is the case in real biological systems. Simulation runs were performed with 8×10^6 integration steps resulting in trajectories that last for 8 ms, which is approximately 5 times the longest membrane time scale $\tau_{M,\max}$. The graphs presented in the following are the results of averaging over a minimum of 500 independent trajectories, where the first 10^6 time steps were not taken into account in order to ensure equilibration of the membrane configuration and the particle position relative to the membrane shape.

B. Effective diffusion coefficient

To test our explicit expression (25), we have performed elaborate simulations using the scheme described in the previous section. In Fig. 1, we present the resulting $D_{\rm eff}/D_0$ as a function of $\rho\gamma$ with the ratio of protein area to system size ρ, Eq. (4), and the ratio of the protein to membrane bending rigidity γ for three different protein mobilities. The detailed parameters of the simulations are given in the figure caption. The comparison of the simulation results and the corresponding analytical expression shows very good agreement for all the chosen parameters. Since the simulations were all performed with $(\beta\kappa)^{-2}=0.04$, we are well within the limits, where we expect our analytical result to hold. These simulation parameters were chosen because they represent realistic parameters for biological systems. We thus conclude that our approach to determining the reduction of the effective diffusion coefficient will be of use in experimental studies.

In the following, we will quantitatively analyze the contributions of the correlation functions entering the effective diffusion coefficient. The mean squared displacement $\langle\Delta\mathbf{R}^2(t)\rangle$ for the diffusing protein is formally given by integrating Eq. (6) twice in time

$$\begin{aligned}\langle\Delta\mathbf{R}^2(t)\rangle &= \int_0^t d\tau\int_0^t d\tau'\langle\partial_\tau\mathbf{R}(\tau)\cdot\partial_{\tau'}\mathbf{R}(\tau')\rangle \\ &= \int_0^t d\tau\int_0^t d\tau'[\mu_p^2\langle\mathbf{f}(\tau)\cdot\mathbf{f}(\tau')\rangle + \langle\boldsymbol{\zeta}(\tau)\cdot\boldsymbol{\zeta}(\tau')\rangle \\ &\quad + \mu_p\langle\mathbf{f}(\tau)\cdot\boldsymbol{\zeta}(\tau')\rangle + \mu_p\langle\boldsymbol{\zeta}(\tau)\cdot\mathbf{f}(\tau')\rangle], \qquad (35)\end{aligned}$$

with the conservative force $\mathbf{f}(t)\equiv-\nabla_{\mathbf{R}}\mathcal{H}[h,\mathbf{R}]$ that the membrane exerts on the protein. Thus the mean squared displacement has several additive contributions. Since the effective diffusion coefficient follows from the slope of the mean-square displacement as a function of time via $\langle\Delta\mathbf{R}^2\rangle \equiv 4D_{\rm eff}^{\rm MSD}t$, also the diffusion coefficient has various additive contributions. In Fig. 2, we display the simulation results for the various parts of the mean squared displacement for a chosen set of parameters. The correlations of the stochastic force acting on the particle lead to a $4D_pt$ behavior as is expected from the fluctuation-dissipation theorem of Eq. (8). As we have argued before, the slope of the particle's mean squared displacement as a function of time is smaller than $4D_p$, hence, one of the additive terms must be negative. However, the force correlations $\langle\mathbf{f}(\tau)\cdot\mathbf{f}(\tau')\rangle$ obviously also lead to an additive contribution, which we find to be quite small for the parameters of our simulations. Due to causality correlations $\langle\mathbf{f}(\tau)\cdot\boldsymbol{\zeta}(\tau')\rangle$ with $\tau\leq\tau'$ must be zero, such that the remaining correlations $\langle\boldsymbol{\zeta}(\tau')\cdot\mathbf{f}(\tau)\rangle$ are the cause of the reduction of the diffusion coefficient, as we clearly see from the simulation results. This contribution expresses the reaction of the membrane to the random force acting on the protein: if the random force moves the particle during a small discrete time step, the interaction of the protein with the membrane will slightly change the shape of the membrane during the next time step such that the system comes closer to the energy minimum. However, it cannot be reached during such a short time, leading to the membrane "pulling back" the protein to its initial position before the random movement. This explains the sign of the corresponding correlation function. An important aspect here is that the membrane shape reacts to the movement of the protein. If the membrane shape evolves independently from the particle position, these correlations do not exist leading to an increase in the effective diffusion coefficient [24,27].

C. Membrane height correlations

In the following, we will elucidate that our simulation results for equal bending rigidity of membrane and protein, $\gamma=1$, agree very well with the analytical expressions given in Eqs. (3) and (33). Furthermore, we will show that the quali-

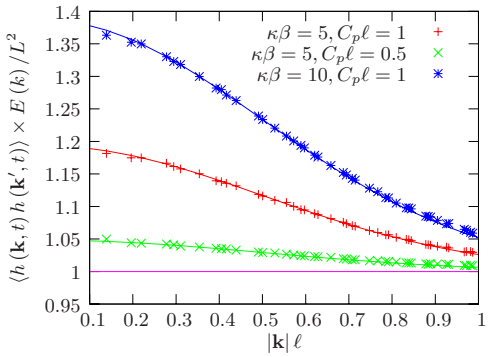

FIG. 3. (Color online) Mean squared height of a membrane with protein normalized by the height correlations of an unperturbed membrane as a function of k for equal bending rigidity of the protein and the membrane, $\gamma=1$. The values for the membrane bending rigidity $\beta\kappa$ and the spontaneous curvature C_p are displayed in the legend. We define $E(k) \equiv (\beta\kappa k^4)^{-1}$.

tative features of these equations are also observed in the more general case $\gamma \neq 1$.

In Fig. 3, we present the height correlation spectrum $\langle h(\mathbf{k})h(-\mathbf{k})\rangle$ as a function of k for $\gamma=1$ and different membrane bending rigidities κ and spontaneous curvatures C_p of the protein. In order to focus on the influence of the protein, we have normalized $\langle h(\mathbf{k})h(-\mathbf{k})\rangle$ by the spectrum of a bare, protein-free membrane. While the symbols represent results from the simulations, the solid lines follow from Eq. (3) using the Gaussian weighting function $G(\mathbf{r}-\mathbf{R})$ given in Sec. II. The influence of the protein is most pronounced for small wave vectors k or large length scales and decreases with increasing k to the value of the bare membrane without protein. Membrane fluctuations on length scales significantly smaller than the inclusion's size are not influenced by the interaction of the protein with the membrane. Comparing simulation results to the analytical expression (3), we find that the agreement is very good as was of course expected. In Fig. 4, we plot the effective bending rigidity $\kappa_{\text{eff}}(k)$ as a function of k as determined from the height correlations that result from simulations with a constant spontaneous curvature C_p and membrane bending rigidity κ, but different bending rigidity ratios γ. For $\gamma=1$, the simulation result agrees

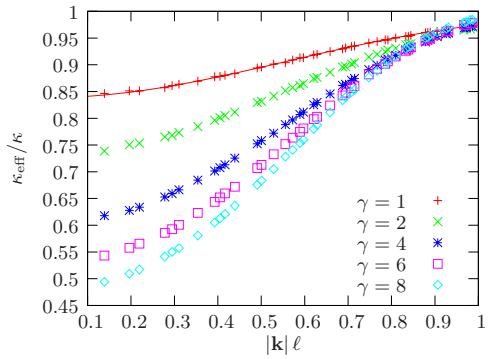

FIG. 4. (Color online) Effective bending rigidity $\kappa_{\text{eff}}(k)$ as a function of k for the given values of γ. The bending rigidity of the membrane is $\beta\kappa=5$ and spontaneous curvature of the protein $C_p\ell = 1$.

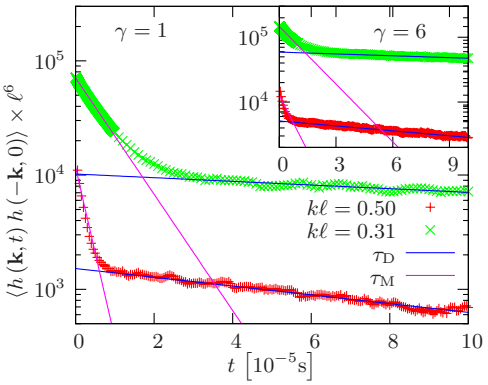

FIG. 5. (Color online) Height correlation functions $\langle h(\mathbf{k},t)h(-\mathbf{k},0)\rangle$ for two arbitrarily chosen k values as a function of time t. The slopes of the solid lines determine the two time regimes dominated by $\tau_M(k)$ for small t and $\tau_D(k)$ for large t.

very well with Eq. (5). With increasing the stiffness of the particle, we find that the qualitative behavior remains similar, however, κ_{eff} is even more reduced. Effectively, an increase in the bending rigidity of the protein leads to a softening of the system. Our results indicate that $\kappa_{\text{eff}}(k)$ saturates with increasing γ. To corroborate this, assumption simulations with even higher γ would need to be performed, but have turned out to be very demanding computationally.

We now turn to the temporal decay of height correlations. In Fig. 5, we display $\langle h(\mathbf{k},t)h(-\mathbf{k},0)\rangle$ as a function of time for two arbitrary wave numbers k. The main plot considers $\gamma=1$, the inset $\gamma=6$. Equation (33) suggests that the two relevant time scales in the system, which are well separated in our calculations, become observable: for small times, the decay is dominated by the membrane time scale $\tau_M(k)$, while for larger times, the decay is predominantly influenced by the movement of the protein and hence the corresponding time scale is $\tau_D(k)$. Regarding the simulation results, we see indeed that the behavior of the correlations is dominated by a fast decay at small times and a slower decrease for large times. While Eq. (33) is an approximate result only for $\gamma=1$, we find that this feature of two dominating time scales is qualitatively also observed for $\gamma \neq 1$. The quantitative fit of the small time behavior with an exponential decay with the characteristic time $\tau_M(k)$ shows very good agreement for both considered values of γ. For $\gamma \neq 1$, the Hamiltonian of the system (2) causes an additional contribution to the inverse characteristic time that depends on γ. However, for the parameters of our simulations, this contribution is obviously negligible.

At large times, the decay is expressed through the time scale $\tau_D(k)$ that is a function of the effective diffusion coefficient D_{eff} of the protein along the membrane. The typical method to identify D_{eff} is to regard the temporal evolution of the mean squared displacement of the protein using the relation $\langle \Delta\mathbf{R}^2\rangle \equiv 4D_{\text{eff}}^{\text{MSD}}t$, as explained above. Using the so-determined value of the diffusion coefficient, we find for large times that the results in Fig. 5 are well approximated by an exponential behavior $\sim\exp[-t/\tau_D(k)]$ for both $\gamma=1$ and $\gamma=6$. Overall, for $\gamma=1$, we observe that the behavior of the height correlations is well described by Eq. (33).

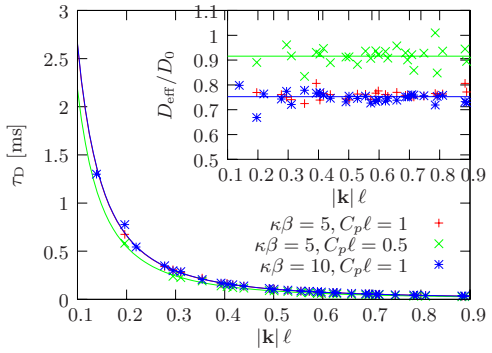

FIG. 6. (Color online) Diffusion dominated decay time $\tau_D(k)$ as a function of k for $\gamma=1$ and the given values for $\beta\kappa$ and C_p. Symbols represent simulation results derived from fitting height correlation functions at later times; solid lines display the theoretical time scale using the effective diffusion coefficient determined through the mean squared displacement of the protein. In the inset, the effective diffusion coefficient determined from the long-time decay using $D_{\rm eff}^M \equiv [k^2\tau_D(k)]^{-1}$ is plotted as a function of k (symbols). Horizontal lines give $D_{\rm eff}^{\rm MSD}$ determined from the mean squared displacement.

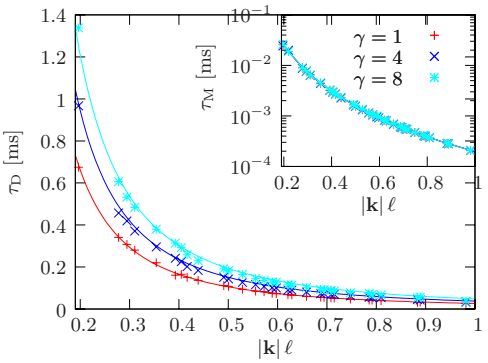

FIG. 7. (Color online) Diffusion time $\tau_D(k)$ as a function of k for the given values of γ. All results apply for $C_p\ell=1$ and $\beta\kappa=5$. Symbols result from simulations while solid lines are given by $(D_{\rm eff}^{\rm MSD}k^2)^{-1}$. Inset shows the corresponding membrane time scale $\tau_M(k)$ determined by fitting the initial decay of the height correlation function (symbols) and given theoretically (solid line).

V. DIFFUSION COEFFICIENT EXTRACTED FROM MEMBRANE SPECTRUM

A. Determination of $D_{\rm eff}$ from simulations

In the discussion of Fig. 5, we used the mean squared displacement to determine the diffusion coefficient of the protein. However, the exponential decay of large time height correlations offers an alternative method to extract $D_{\rm eff}$. The $\tau_D(k)$ resulting from exponential fits to the late time decay as a function of k are plotted in the main graph of Fig. 6 for $\gamma=1$ but different κ and C_p. Using the previously determined value for the diffusion coefficient, we find a good agreement with $\tau_D(k)=(k^2D_{\rm eff}^{\rm MSD})^{-1}$ (solid lines). Thus without prior information on the mean squared displacement of the proteins, it is possible to identify $D_{\rm eff}$ from the height correlations of the membrane using the behavior of $\tau_D(k)$ as a function of the wave number k. In the inset of Fig. 6, we plot $D_{\rm eff}^M \equiv [k^2\tau_D(k)]^{-1}$ as a function of k. We find that the resulting diffusion constant agrees very well with the diffusion constant $D_{\rm eff}^{\rm MSD}$.

While Fig. 6 only considers $\gamma=1$, we will now show that the characteristic time scales τ_M and τ_D can also be identified for $\gamma\neq 1$. The inset of Fig. 7 displays $\tau_M(k)$ as a function of k as determined from the exponential decay of the height correlations at short times for different values of γ. Apart from γ, the other parameters of the membrane and the particle are kept constant. We find that the results do not depend on the rigidity of the protein. The dominant time scale for short times is only determined by the properties of the membrane and coincides with the correlation time of a freely fluctuating membrane without protein. In the main plot, the late time diffusive time scale τ_D is plotted as a function of k. These results clearly depend on the rigidity of the protein, but only because the diffusive motion is influenced by the protein-membrane interaction. If we determine the effective diffusion coefficient from the mean-square displacement and compare the thus calculated τ_D (solid lines) to the simulation results from the late time exponential fits to the height correlations (symbols), the agreement is again very good. Thus, if we had not had the possibility to determine the mean squared displacement of the protein, we could have determined $D_{\rm eff}$ solely from the time dependence of the height correlations.

B. Estimate of experimental feasibility

In the following, we will show that our suggested method to determine the lateral diffusion coefficient of proteins from height fluctuations in a membrane is experimentally feasible. Height correlation functions can be determined by video microscopy as explained in the introduction. If $\tau_{\rm co}(k)$ is the crossover time from the decay of correlations caused by the membrane dynamics to that dominated by the diffusive time scale of the proteins, experiments must meet two conditions in order for the crossover to become observable: on the one hand, $\tau_{\rm co}(k)$ must be larger than the temporal resolution of the camera used in the experiment. Values given in previous studies [15] are on the order of 0.03 s. On the other hand, $\tau_{\rm co}(k)$ must be smaller than the experimentally accessible total time that is on the order of minutes. Since the crossover time is a function of the wave vector, the restrictions for $\tau_{\rm co}(k)$ must, furthermore, be fulfilled for experimentally accessible wave numbers. The spatial resolution of video microscopy allows for k values smaller than approximately 4 $\mu{\rm m}^{-1}$.

If we have a general time-dependent function of the form $A\exp(-at)+B\exp(-bt)$, with $a \gg b$, a good estimate for the crossover time is given by $(A+B)\exp(-a\tau_{\rm co})=B\exp(-b\tau_{\rm co})$. Within our model, the crossover time for $\gamma=1$ is given by

$$\tau_{\rm co}(k) \equiv \left[\frac{1}{\tau_M(k)} - \frac{1}{\tau_D(k)}\right]^{-1} \ln\{1 + [\beta\kappa\rho\pi a_p^2 C_p^2 G(\mathbf{k})G(-\mathbf{k})]^{-1}\}. \quad (36)$$

While lateral diffusion coefficients of proteins in membranes are on the order of 10^{-8} cm^2/s [11], the spontaneous curva-

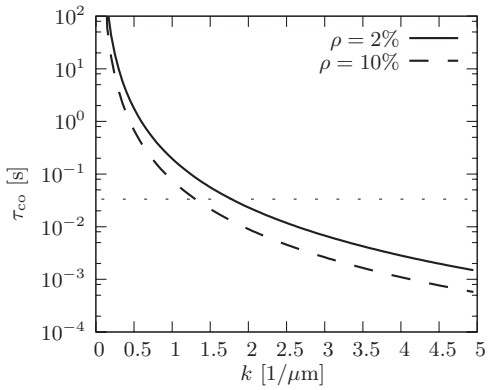

FIG. 8. Crossover time $\tau_{co}(k)$ from membrane fluctuation to diffusion-dominated decay of height correlations as a function of wave number k [see Eq. (36)] for $\gamma=1$, $D_{eff}=10^{-8}$ cm^2/s, $\sqrt{\pi}a_pC_p=1$, and $\beta\kappa=10$. Dotted line corresponds to the typical resolution time of video microscopy.

ture is not so well determined. In Fig. 8, we display the crossover time $\tau_{co}(k)$ as a function of the wave number for different protein densities ρ and $D=10^{-8}$ cm^2/s, $\beta\kappa=10$, and $\sqrt{\pi}a_pC_p=1$. For the regarded protein densities, we find that for small wave numbers, τ_{co} becomes larger than the typical temporal resolution of experiments. We find that for wave numbers that lie within the experimental range, it should be possible to observe the two characteristic time scales. Thus, the determination of the lateral diffusion coefficient from the diffusion dominated decay of membrane height correlations should be feasible. However, the interesting wave-number range is reasonably narrow, since τ_{co} is strongly increasing for smaller k. Note that Eq. (36) is only valid for the situation of equal bending rigidity of the protein and the membrane. In general, this is obviously not the case, however, the height correlations displayed in Fig. 5 for $\gamma \neq 1$ let us assume that the crossover time is only weakly influenced by the bending rigidity of the protein and that our estimate remains valid.

VI. CONCLUSIONS

In this paper, we have considered the influence of a protein interacting with a fluctuating membrane via its bending rigidity and spontaneous curvature on both the dynamics of the protein and the membrane. The quantities we have looked at in details are the lateral diffusion coefficient of the protein and the height correlations of membrane fluctuations by use of analytical calculations and Langevin simulations. We argue that the lateral diffusion coefficient of a protein that interacts with the membrane is always reduced compared to its bare diffusion coefficient as long as there are no external driving forces or active processes. Using a path-integral approach, we could derive an analytical expression for this reduction that is valid within the lowest order of a $(\beta\kappa)^{-1}$ expansion. Our simulations with parameters that resemble those of real experiments show a wide applicability of this expression. In addition, a closer look at the correlation functions that contribute to the reduction of the diffusion coefficient shows that the correlations between the stochastic force acting on the protein and the response of the membrane to the movement of the protein are responsible for the reduction.

The diffusion of the protein is obviously correlated with the height correlations of the membrane. The determination of the height correlations for the case of equal bending rigidity of the protein and the membrane reveals that the protein-membrane interaction has a significant influence compared to a free membrane. The most predominant feature is that the temporal decay of correlations does not only display the time scale one would expect from the membrane, but that the diffusive time scale of the influencing protein becomes important. In realistic biomembrane systems, these two time scales are well separated such that a crossover from the initially fast decay of membrane fluctuations to the slower protein diffusion dominated decay is likely to be observed in experiments. Since the decay at later times is directly related to the effective diffusion coefficient of the protein, we suggest that the measurement of membrane fluctuations might actually provide a means to determine the lateral diffusion coefficient of the inserted proteins.

Our systematic approach to lateral diffusion of a protein interacting with the shape of the membrane and the related influence on the membrane fluctuation spectrum can be extended in various directions. The first question arising from our study is to work out corrections to the $(\beta\kappa)^{-1}$ expansion and to estimate their relevance. A further perspective resulting from our analysis is the interesting limit $\Lambda/\mu_0 \to 0$ when the protein effectively moves in a fixed membrane configuration. This situation is interesting theoretically, since the diffusing particle no longer "drags along" the membrane, but is hindered in its movement by potential barriers caused by the interaction of the particle with the membrane. Finally, while we have so far only considered membranes that are on average flat, the extension to ruffled membranes poses an interesting challenge with significant relevance for biological membranes such as the endoplasmic reticulum or the cristae in mitochondria.

ACKNOWLEDGMENT

We thank Thomas Speck for many helpful discussions.

[1] B. Alberts, D. Bray, J. Lewis, M. Raff, K. Roberts, and J. D. Watson, *Molecular Biology of the Cell* (Garland, New York, 1994).
[2] S. Chiantia, J. Ries, and P. Schwille, BBA-Biomembranes **1788**, 225 (2009).
[3] P. H. M. Lommerse, H. P. Spaink, and T. Schmidt, BBA-Biomembranes **1664**, 119 (2004).
[4] E. A. J. Reits and J. J. Neefjes, Nat. Cell Biol. **3**, E145 (2001).
[5] C. W. Cairo and D. E. Golan, Biopolymers **89**, 409 (2008).
[6] H. Lamb, *Hydrodynamics* (University Press, Cambridge, 1959).
[7] P. G. Saffman and M. Delbrück, Proc. Natl. Acad. Sci. U.S.A. **72**, 3111 (1975).
[8] R. Peters and R. J. Cherry, Proc. Natl. Acad. Sci. U.S.A. **79**, 4317 (1982).
[9] C. C. Lee, M. Revington, S. D. Dunn, and N. O. Petersen, Biophys. J. **84**, 1756 (2003).
[10] P. Cicuta, S. L. Keller, and S. L. Veatch, J. Phys. Chem. B **111**, 3328 (2007).
[11] Y. Gambin, R. Lopez-Esparza, M. Reffay, E. Sierecki, N. S. Gov, M. Genest, R. S. Hodges, and W. Urbach, Proc. Natl. Acad. Sci. U.S.A. **103**, 2098 (2006).
[12] G. Guigas and M. Weiss, Biophys. J. **91**, 2393 (2006).
[13] T. Charitat, S. Lecuyer, and G. Fragneto, BioInterphases **3**, FB3 (2008).
[14] J. F. Faucon, M. D. Mitov, P. Méléard, I. Bivas, and P. Bothorel, J. Phys. (France) **50**, 2389 (1989).
[15] J. Pecreaux, H. Döbereiner, J. Prost, J. Joanny, and P. Bassereau, Eur. Phys. J. E **13**, 277 (2004).
[16] R. Rodríguez-García, L. R. Arriaga, M. Mell, L. H. Moleiro, I. López-Montero, and F. Monroy, Phys. Rev. Lett. **102**, 128101 (2009).
[17] U. Seifert and S. A. Langer, Europhys. Lett. **23**, 71 (1993).
[18] V. Vitkova, P. Méléard, T. Pott, and I. Bivas, Eur. Biophys. J. **35**, 281 (2006).
[19] P. Girard, J. Prost, and P. Bassereau, Phys. Rev. Lett. **94**, 088102 (2005).
[20] M. D. El Alaoui Faris, D. Lacoste, J. Pécréaux, J.-F. Joanny, J. Prost, and P. Bassereau, Phys. Rev. Lett. **102**, 038102 (2009).
[21] U. Seifert, Adv. Phys. **46**, 13 (1997).
[22] M. Goulian, R. Bruinsma, and P. Pincus, Europhys. Lett. **22**, 145 (1993).
[23] R. R. Netz and P. Pincus, Phys. Rev. E **52**, 4114 (1995).
[24] E. Reister and U. Seifert, Europhys. Lett. **71**, 859 (2005).
[25] E. Reister-Gottfried, S. M. Leitenberger, and U. Seifert, Phys. Rev. E **75**, 011908 (2007).
[26] A. Naji and F. L. H. Brown, J. Chem. Phys. **126**, 235103 (2007).
[27] S. M. Leitenberger, E. Reister-Gottfried, and U. Seifert, Langmuir **24**, 1254 (2008).
[28] N. S. Gov, Phys. Rev. E **73**, 041918 (2006).
[29] R. Shlomovitz and N. S. Gov, Europhys. Lett. **84**, 58008 (2008).
[30] A. Naji, P. J. Atzberger, and F. L. H. Brown, Phys. Rev. Lett. **102**, 138102 (2009).
[31] S. Leibler, J. Phys. (France) **47**, 507 (1986).
[32] I. Bivas and P. Méléard, Phys. Rev. E **67**, 012901 (2003).
[33] F. Divet, T. Biben, I. Cantat, A. Stephanou, B. Fourcade, and C. Misbah, Europhys. Lett. **60**, 795 (2002).
[34] R.-J. Merath and U. Seifert, Phys. Rev. E **73**, 010401(R) (2006).
[35] The effect of the membrane curvature on the protein mobility derived from the projected flat trajectory in the (x,y) plane is well described within a preaveraging approximation that integrates out the membrane fluctuations. The μ_p used in Eq. (6) resembles the projected, preaveraged mobility related to the actual mobility $\mu \equiv D_0/k_BT$ along the membrane through $\mu_p/\mu=(1+\langle g^{-1}\rangle)/2$, with the metric $g \equiv 1+[\partial_x h(\mathbf{r})]^2 +[\partial_y h(\mathbf{r})]^2$ [25].
[36] S. Lifson and J. L. Jackson, J. Chem. Phys. **36**, 2410 (1962).
[37] P. Reimann, C. Van den Broeck, H. Linke, P. Hänggi, J. M. Rubi, and A. Pérez-Madrid, Phys. Rev. E **65**, 031104 (2002).
[38] H. Risken, *The Fokker-Planck Equation: Methods of Solutions and Applications*, Springer Series in Synergetics (Springer, New York, 1996).
[39] L. C.-L. Lin and F. L. H. Brown, Phys. Rev. Lett. **93**, 256001 (2004).
[40] L. C.-L. Lin and F. L. H. Brown, Phys. Rev. E **72**, 011910 (2005).
[41] F. L. Brown, Annu. Rev. Phys. Chem. **59**, 685 (2008).
[42] M. Frigo and S. G. Johnson, Proc. IEEE **93**, 216 (2005).